

Comparing Different Settings of Parameters Needed for Pre-processing of ECG Signals used for Blood Pressure Classification

Monika Simjanoska¹, Gregor Papa², Barbara Koroušić Seljak² and Tome Eftimov²

¹Faculty of Computer Science and Engineering, Ss. Cyril and Methodius University,
Rugjer Boshkovikj 16, 1000 Skopje, Macedonia

²Computer Systems Department, Jožef Stefan Institute, Jamova cesta 39, 1000 Ljubljana, Slovenia

Keywords: Biomedical Signal Analysis, ECG, Signal Length, Baseline Removal, Blood Pressure Classification.

Abstract: Because a real-time monitoring using electrocardiogram (ECG) signals is a challenging task, the pre-processing techniques used for ECG signal analysis are crucial for obtaining information that is further used for some more complex analysis, such as predictive analyses. We compared different settings of parameters needed for pre-processing of ECG signals in order to estimate the valuable information that can be further used for blood pressure classification. Two parameters were involved in the comparison: i) the signal length used for ECG segmentation; and ii) the cut-off frequency used for baseline removal. The first parameter is the parameter used for obtaining ECG segments that are further used, and the second one is the frequency used for baseline removal. Thirty different combinations, each a combination of a signal length and a cut-off frequency, were evaluated using a dataset that contains data from five commercially available ECG sensors. For signal lengths: 10 s, 20 s, and 30 s, were used for data segmentation, while the cut-off frequency for baseline removal starts from 0.05 Hz, till 0.50 Hz, with a step length of 0.05 Hz. The evaluation of these combinations was done in combination with complexity analysis used for features extraction that are further used for blood pressure classification. Experimental results, obtained using a data-driven approach by comparing the combinations using the results obtained from the classification for 17 performance measures, showed that a signal length of 30 s carries the most information in a combination with cut-off frequency between 0.10 Hz and 0.20 Hz. Results contribute to the arguments published in the literature discussing the optimal ECG sample lengths needed for building predictive models, as well as the lower frequencies where the ECG components overlap with the baseline wander noise.

1 INTRODUCTION

A biomedical processing system includes a biological system of interest, sensors used to follow the physiological conditions, and a methodology for biomedical signal analysis in order to extract the useful information from the system. In this paper, the biological system addressed is the heart system, and its electrical activity is followed using electrocardiogram (ECG) signals. Through ECG we want to follow blood pressure. Two phases for managing blood flow exist: i) a diastole phase known as the *filling phase* and ii) a systole phase known as the *pumping phase*. The blood pressure (BP) is defined as the force of the blood pushing against the walls of the arteries as the heart pumps blood (Shriram et al., 2010).

Nowadays, commercially available wearable biosensors (e.g., ECG sensors, sweating-rate sensors, respiration-rate body sensors) provide an opportunity

for real-time monitoring of human vital signs, which further helps the process of preventive, timely notification and real-time diagnosis (Cosoli et al., 2015). Recently, many systems for non-invasive BP monitoring have been developed, such as: i) the Superficial Temporal Artery Tonometry-based device (Sackl-Pietsch, 2010), ii) the PPG optical sensor (Canning et al., 2016), iii) ARTSENS (ARTerial Stiffness Evaluation for Non-invasive Screening) for brachial arterial pressure (Mouradian et al., 2015), iv) an electronic system based on the oscillometric method (Sahani et al., 2014), v) a BP estimation device based on the principle of volume compensation (Marani and Perri, 2012), vi) a Modulated Magnetic Signature of Blood mechanism (Tanaka et al., 2007), and vii) portable equipment that includes a cuff-based BP sensing system (Li et al., 2013). However, they are specialized only for BP measurements, and exclude

the other vital signs.

The data collected from sensors that measure ECG signal as physiological signal can be further used for developing smart phone applications for real-time diagnosis (Cosoli et al., 2015). In (Simjanoska et al., 2018), the relation between the ECG signal and BP using supervised machine learning (ML) approaches has been investigated. For this reason, a pre-processing that involves ECG signal complexity analysis was applied in order to extract features that are further used for training a meta-model used for blood pressure classification. The ECG signal analysis was performed using a signal length of 30 s and a band-pass Butterworth filter with a frequency of 0.30 Hz for removing the baseline wander without deforming the ECG signal. These parameters (30 s; 0.03 Hz) were chosen following the state-of-the-art literature. Using such setting, promising results were achieved that indicate the relation between the complexity features of the ECG signals and the BP.

However, in real-life scenarios (e.g., civil and military emergency situations) there is no guaranty that there will be enough time to measure long ECG samples. For this reason, in this study we focus on comparison of different combinations of parameters for signal length and frequency used for baseline removal (i.e. different ECG signal analysis) and their influence on the end result of the methodology used for BP classification. We consider signal lengths of 10 s, 20 s, and 30 s, and frequency starting from 0.05 Hz, till 0.50 Hz, with a step length of 0.05 Hz. The novelty is also in the evaluation of the influence, in which we did not use only one performance measure, but a set of performance measures with a data-driven approach in order to make a general conclusion.

In the remainder of the paper, we first present an overview of the related work. Then we present the methodology used for comparison of the parameters values used for pre-processing of ECG signals is explained in detail, followed by the experimental results and discussion. Finally, the conclusions of the paper are presented followed by directions for future work.

2 RELATED WORK

Most of the recently published studies on BP estimation use a combination of ECG and photoplethysmogram (PPG) sensors (Sahoo et al., 2011; Ilango and Sridhar, 2014; Thomas et al., 2016). The common techniques for obtaining measurements on BP mainly rely on Pulse Wave Velocity (PWV), Pulse Arrival Time (PAT), and Pulse Transit Time (PTT) (Choi et al., 2013; Goli and Jayanthi, 2014; Nye et al., 2015;

Seo et al., 2015), all of which require an accurate PPG measurement, which is not simple to get unobtrusively yet, and no clear proof on the PPG measurement's relation to the BP has been provided (Payne et al., 2006; Wong et al., 2009; i Carós, 2011). The relationship between the ECG signal and BP estimation has been discussed in (Chan et al., 2001; Ahmad et al., 2012). Both methods used an additional PPG sensor with an ECG sensor. The results from several studies that address the ECG-BP relationship (Schroeder et al., 2003; Hassan et al., 2008) confirm that no strong relationship exists between hypertension occurrence and morphological changes in ECG. For this reason, in (Simjanoska et al., 2018), instead of using morphological changes in ECG, complexity analysis was used to detect bio-system complexity. For this reason, the ECG signals were segmented using signal length of 30 s, for which cut-off frequency of 0.30 Hz was applied for baseline removal.

3 METHODOLOGY

To compare different combinations of parameters used for pre-processing of ECG signals, we propose an approach, which goes through four different levels: data segmentation and baseline removal, feature extraction, classification, and classifiers ranking.

- *Level 1:* The key part is the **data segmentation and baseline removal**, because the end result is comparing different parameters that are used for obtaining ECG segments that are further used for blood pressure classification. For this reason, 30 different combinations were included, a signal length of 10 s, 20 s, and 30 s, and frequency for baseline removal starting from 0.05 Hz, till 0.50 Hz, with a step length of 0.05 Hz.
- *Level 2:* To compare the different combinations, for each of them the same complexity analysis was applied for **feature extraction**.
- *Level 3:* The extracted features for each combination are further used to learn a **classification** model for blood pressure following the stacking procedure.
- *Level 4:* Finally, by performing **classifiers ranking** using a set of different performance measures, the influence of each combination can be estimated.

The flowchart of the methodology is presented in Figure 1. Further, each level is explained in more detail.

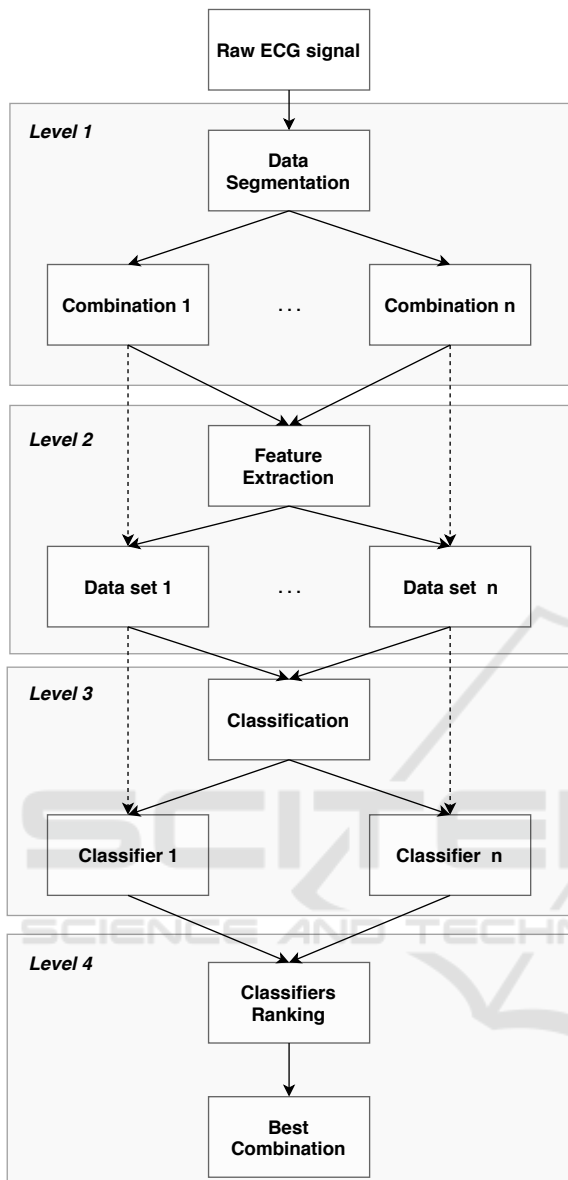


Figure 1: The flowchart of the methodology.

3.1 Data Segmentation and Baseline Removal

The raw ECG signals are segmented using signal lengths of 10 s, 20 s, and 30 s. In the process of segmentation, the segments were also labeled with the appropriate BP class. The result of this are three data sets, the first consists of segments of 10 s, the second consists of segments of 20 s, and the third of segments of 30 s. Further, a band-pass filter is applied on each of these datasets in order to preserve only valid ECG information. The cut-off frequency for baseline removal starts from 0.05 Hz, till 0.50 Hz, with

a step of 0.05 Hz. Performing 10 cut-off frequencies on each dataset, it results in 30 data sets, which were further called “combinations” because each of them is described with a combination of signal length and cut-off frequency.

3.2 Feature Extraction

After creating 30 datasets (combinations), each of them is used for feature extraction, in which the problem is addressed from the perspective of complexity analysis (Eke et al., 2002; Morabito et al., 2012; McBride et al., 2014), and not as other traditional approaches in which morphological features are used (Wong et al., 2009; Zhang and Zhang, 2006; Nitzan, 2011). For this reason, for each dataset, five complexity metrics are calculated: signal mobility, signal complexity, fractal dimension, autocorrelation, and entropy.

3.2.1 Signal Mobility

Given $x_i, i = 1, \dots, N$ is the ECG signal of length N and $d_j = x_{j+1} - x_j$ is the first-order variation in the signal, then the first-order factors, S_0 and S_1 , are calculated as:

$$S_0 = \sqrt{\frac{\sum_{i=1}^N x_i^2}{N}} \quad (1)$$

$$S_1 = \sqrt{\frac{\sum_{j=2}^{N-1} d_j^2}{N-1}} \quad (2)$$

The signal mobility quantitatively measures the level of variation in the signal. It is calculated as a ratio between the factors S_1 and S_0 :

$$Mobility = \frac{S_1}{S_0}, \quad (3)$$

3.2.2 Signal Complexity

Given the first-order variation of the ECG signal $d_j, j = 1, \dots, N-1$, the second-order variation of the signal is presented by $g_k = d_{k+1} - d_k$. Then, the second-order factor is calculated as:

$$S_2 = \sqrt{\frac{\sum_{k=3}^{N-2} g_k^2}{N-2}}, \quad (4)$$

Both the signal mobility and signal complexity were computed by using the Hjorth parameters method (Kugiumtzis and Tsimpiris, 2010).

3.2.3 Fractal Dimension

Fractal dimension measures the self-similarity of the signal. By zooming and comparing different portions, it describes fundamental patterns hidden in the signal. Higuchi algorithm (Monge-Álvarez, 2015) has been used to calculate the fractal dimension. The method works with a set of k subseries with different resolutions, creating a new time series X_k , for $m = 1, \dots, k$:

$$X_k^m : x(m), x(m+k), x(m+2k), \dots, x(m + \lfloor \frac{N-m}{k} \rfloor k) \quad (5)$$

The length of the curve X_k^m , $l(k)$ is calculated as:

$$l(k) = \frac{(\sum_{i=1}^{\lfloor \frac{N-m}{k} \rfloor} |x(m+ik) - x(m+(i-1)k)|)(N-1)}{(\lfloor \frac{N-m}{k} \rfloor)k} \quad (6)$$

Then, for each k in range 1 to k_{max} , the average length is calculated as the mean of the k lengths $l(k)$ for $m = 1, \dots, k$. The fractal dimension is the estimation of the slope of the plot $\ln(l(k))$ vs. $\ln(1/k)$.

3.2.4 Autocorrelation

The similarity between the signal and its shifted version is measured via autocorrelation. Let τ be the amount of shift, and then the autocorrelation is calculated as:

$$r_{xx}(\tau) = \int_{-\inf}^{+\inf} x(t)x(t-\tau)p_{xx}(x(t),x(t-\tau))dt, \quad (7)$$

where $p_{xx}(x(t),x(t-\tau))$ presents the joint probability density function of $x(t)$ and $x(t-\tau)$.

3.2.5 Entropy

Entropy expresses the randomness of the signal. The decrease of entropy often indicates a disease (Zhou et al., 2017). The amount of information is expressed through the concept of probability. Let p_i denote the probability of each outcome x_i within the ECG signal X for $i = 1, \dots, N-1$. Then, entropy is calculated as:

$$Entropy = \sum_{i=0}^{N-1} p_i \log\left(\frac{1}{p_i}\right) \quad (8)$$

3.3 Classification

Performing the feature extraction for each of the 30 datasets (combinations), each of them is used to train a meta-model that will be used to predict the BP class. The performance of the meta-model on each data set is used to compare different signal lengths and cut-off frequencies. The methodology that is applied is

taken from a previous study (Simjanoska et al., 2018), where the meta-model was learned for a signal length of 30 s and cut-off frequency of 0.30 Hz. Using this combination, it was shown that promising results can be achieved.

The meta-model follows a stacking design, in which seven different classifiers are used: Bagging (Breiman, 1996), Boosting (Freund et al., 1996), SVM (Hearst et al., 1998), K-means (Liao and Vemuri, 2002), Random Forest (Liaw et al., 2002), Naive Bayes (Rish et al., 2001), and J48 (Patil and Sherekar, 2013). The probabilities from each of them for all the feature vectors to belong in each class, comprise a new feature vector upon which a META classifier (Random Forest) is trained. More details about the classification methodology are provided in (Simjanoska et al., 2018).

3.4 Ranking of Classifiers

For each dataset (combination), a meta-model is trained using a training set and it is evaluated on a corresponding validation set. For this reason, each dataset is m -times split into training and validation set, since we have multiple **independent measurement** for each subject (i.e. participant) and as the **number of measurements varies for each subject**. We follow the rule that if a subject is included in one set, none of its measurements may occur in another set. So for each combination, m meta-models are trained.

To evaluate the performance of the meta-models trained for each combination of signal length and cut-off frequency, we used an ensemble (a fusion) of a set of 17 performance metrics:

- **Accuracy (ACC)** - represents the fraction between the number of correct predictions by the total number of predictions made.
- **Cohen's Kappa** - compares the observed accuracy (the number of correctly classified instances) with the expected accuracy (taking into account the number of instances in each class, along with the number of instances that the classifier agreed with the ground truth label).
- **Precision (PR)** - captures the effect of the large number of negative examples on the classifier's performance, by comparing false positives (FP) to true positives (TP) rather than true negatives (TN), i.e. it measures how many of the predicted instances were TP.
- **Recall (RC)** - to measure how many of the TP instances were predicted.

- **F-Measure** - measures the trade-off between recall and precision giving equal importance to recall and precision.
- **Area Under PRC** - precision-recall curve does not account for TN, since TN is not a component of either Precision or Recall. Given there are more negatives (normal) than positives (hypertension), PRC might be a very informative evaluation metric of the performance of the classifier. Having a model at the upper right corner, means that the classifier gets only the TP with no FP and no false negatives (FN) at all and thus is a perfect classifier.
- **Area Under ROC** - the ROC curve plots the True Positive Rate (TPR) vs. False Positive Rate (FPR). Therefore achieving a model at the upper left corner, means that the classifiers is getting no FP at all and thus is a perfect classifier.
- **Matthews Correlation (COR)** - takes the advantage from all four metrics TP, FP, TN and FN to calculate the correlation coefficient between the observed and predicted classifications (Vihinen, 2012).
- **Relative Absolute Error (RAE)** - is an error measure relative to a simple predictor, meaning it takes the total absolute error and normalizes it by dividing it by the one of the simple predictor.
- **Root Relative Squared Error (RRSE)** - takes the total squared error and normalizes it by dividing by the total squared error of the simple predictor. The square root reduces the error to the same dimensions as the problem at hand.
- **Root Mean Squared Error (RMSE)** - explains the standard deviation of the prediction error.
- **Informedness (INF)** - quantifies how informed a classifier is for the specified class. It provides insight into how consistently the classifier predicts the class (Powers, 2011).
- **Markedness (MAR)** - quantifies how marked a class is for the specified classifier, i.e. how consistently the class has the classifier as a marker by combining measures about correct classifications (Powers, 2011).
- **Micro F-measure (MF)** - aggregates the contributions of all classes to compute the average F-measure by considering the total TPs, FNs and FPs.

Table 1: Decision matrix.

	q_1	q_2	\dots	q_{17}
C_1	$q_1(C_1)$	$q_2(C_1)$	\dots	$q_{17}(C_1)$
C_2	$q_1(C_2)$	$q_2(C_2)$	\dots	$q_{17}(C_2)$
\vdots	\vdots	\vdots	\vdots	
C_{30}	$q_1(C_{30})$	$q_2(C_{30})$	\dots	$q_{17}(C_{30})$

- **Log Likelihood (LL)** - presents the probability of the observed prediction given the real class.
- **Mutual Information (MI)** - measures whether the real and the predicted labels are statistically depended.
- **Pearson's Chi-squared Test (PRS)** - to measure whether the observed and expected frequencies are the same by comparing the predicted contingency table to an expected table.

To compare the results of the meta-models obtained for each combination using a set of performance measures, their results are organized into a decision matrix (Table 1). The rows of the decision matrix correspond to different meta-models and the columns correspond to the values obtained for the performance measures. First, a generalized preference function should be selected for each performance measure. In our case, the V-shape generalized preference function is used for each performance measure, where the threshold of strict preference is set to the maximum difference that exists for each preference measure from all pairwise comparisons according to that performance measure (Brans and Mareschal, 2005). After that, the average preference index for each pair of meta-models should be calculated, which gives information of global comparison between them using all performance measures. To rank the meta-models, a net flow for each one needs to be calculated. It is a difference between a positive preference flow and a negative preference flow of the meta-model. The positive preference flow gives information about how a given meta-model is globally better than the other meta-models, while the negative preference flow gives the information about how a given meta-model is outranked by all the other meta-models. This approach has already been used for evaluation of multi-objective meta-heuristic stochastic optimization algorithms regarding a set of performance measures. More details about the ranking approach and the equations for the net, positive, and negative flow, can be found in (Eftimov et al., 2018).

4 EVALUATION

4.1 Data Collection from Multiple Sensors

The data was collected using five ECG sensors, from which four are commercially available ECG sensors (Hacks, 2015; Biosignals, 2016; Technology, 2017; Trobec et al., 2018a) and one is from the online available Physionet database (Goldberger et al., 2000). For each ECG signal, reference SBP and DBP values are attached, which are measured in parallel using electronic sphygmomanometer. The information about each sensor, its reliability, the number of participants measured by each sensor, and their age, is presented in Table 2. All the human subjects involved in the research signed an agreement allowing their ECG data to be used for research goals. The involved participants come from different age and health status, and the measurements were performed in moving and sitting positions. The patients included from the Physionet database are explicitly selected to suffer brain injuries.

As we mentioned before, each ECG signal is accompanied with SBP and DBP values, we also added the BP class, which is the target in the classification. To obtain the BP class for each ECG measurement, a publicly available scheme presented in Table 3 (Program et al., 2004; AHA, 2016) was used. The BP classes seem not to be mutually exclusive, however this was solved by giving priority to the more severe BP conditions by checking the “AND” conditions at the end of the ECG samples mapping procedure. To solve the imbalanced-class data, BP classes were grouped into three main categories: hypotension (HPTN) and normal (N) as Normal class (denoted as 0); prehypertension (PHTN) as Prehypertension class (denoted as 1); and stage 1 hypertension (S1HTN), stage 2 hypertension (S2HTN), isolated systolic hypertension (ISHTN), and hypertensive crisis (HTNC) as Hypertension class (denoted as 2).

4.2 Data Segmentation and Baseline Removal

After the data from all sensors was collected and labeled with an appropriate BP class, data segmentation was applied on each ECG signal. The raw ECG signals were segmented using signal lengths of 10 s, 20 s, and 30 s, and each of the signal length was analyzed with different cut-off frequency for baseline removal starting from 0.05 Hz, till 0.50 Hz, with a step of 0.05 Hz. The segments were labeled with the BP class

from the corresponding ECG signal from which they are obtained. Finally, we create 30 different combinations that should be analyzed in the case of BP classification in order to provide information about which pre-processing combination gives the most promising results.

4.3 Feature Extraction

For each of 30 datasets (i.e. combinations), we extracted the five complexity features that will be further used for learning a meta-model used for BP classification. Each of the datasets is described with the same five features, however the features values are different due to different signal length and cut-off frequency for baseline removal that are used.

4.4 Classification

Having the 30 datasets, for each one the classification was done using a previously published methodology that follows a stacking design (Simjanoska et al., 2018). Output probabilities from seven different classifiers, already mentioned above, were used as features to train a meta-model for multi-class BP classification using Random Forest. In our case, the number of classes is three.

4.5 Ranking of Classifiers

To evaluate the performance of each meta-model obtained for each dataset (combinations), we follow the idea of splitting the datasets into training and validation set. The splitting is made in a way that if a subject is included in the training set, none of its measurements may occur in the validation set, and vice versa. For this reason and in order to build a robust model for each combination, each dataset was split 30 times into training and validation sets. We followed the rule of 75% of the subjects were used for training and 25% of the subjects were used for validation.

Using this approach, for each combination we obtained 30 different meta-models and their evaluation on the corresponding validation sets described by the 17 performance measures. The evaluation was performed in two scenarios.

First, within each configuration, we used the ranking scheme based on PROMOTHEE method in order to find the best split for each combination, which results in the best meta-model for each combination. Further, the best meta-models for all combinations were again evaluated with the same ranking scheme and the set of 17 performance measures in order to obtain the most promising combination of

Table 2: Sensors summary information.

Dataset	Reliability	Participants	Age
Cooking hacks (Hacks, 2015)	(Winderbank-Scott and Barnaghi, 2017)	16	16–72
180° eMotion FAROS (Biosignals, 2016)	(Ahonon et al., 2016)	3	25–27
Zephyr Bioharness module (Technology, 2017)	(Johnstone et al., 2012)	14	20–73
Savvy sensor platform (Trobec et al., 2018a)	(Trobec et al., 2018b)	21	15–54
Charis Physionet database (Goldberger et al., 2000)	(Kim et al., 2016)	7	20–74

Table 3: Rules and categorization.

Joined class	Class	SBP (mmHg)	Logical	DBP (mmHg)
Normal	HPTN	<=90	OR	<=60
	N	90–119	AND	60–79
Prehypertension	PHTN	120–139	OR	80–89
	SIHTN	140–159	OR	90–99
Hypertension	S2HTN	>=160	OR	>=100
	ISHTN	>=140	AND	<90
	HTNC	>=180	OR	>=110

pre-processing that was applied. The performance of the best meta-model within each configuration are presented in Table 4. The first column presents the parameters settings for each combination. The last column reported the ranking for each combination, which is obtained by the ranking scheme when the best meta-models from all combinations are compared.

Using the information reported in Table 4, we can see that the best results are obtained using the meta-model for the combination with the signal length of 10 s and cut-off frequency for baseline removal 0.30 Hz, the second best is obtained for the signal length of 20 s and the cut-off frequency of 0.45 Hz, and the third with the signal length of 30 s and the cut-off frequency of 0.15 Hz. From here, there is no general conclusion for which data segmentation provides the most valuable information for BP classification; however there is a question of the robustness of the results, or if selecting the best meta-model (or best splitting) for each combination corresponds to a real-life application.

Second, in order to have more robust results, the results from 30 splits for each combination were aggregated by averaging the results for each performance measure separately, and the average value for each performance measure was further used for each combination. This was made with the purpose of following the cross-validation idea. Then, the 30 combinations were compared using the ranking scheme and the set of 17 performance measures. The averaged performance for each configuration is presented in Table 5. The first column presents the parameters settings for each combination. The last column reported the ranking for each combination, which is ob-

tained by the ranking scheme when all combinations are compared using the averaged results.

Using the results reported in Table 5, it follows that the best meta-model can be learned using the signal length of 30 s and cut-off frequency of 0.10 Hz, the second best can be learned using the signal length of 30 s and the cut-off frequency of 0.15 Hz, and the third with the signal length of 30 s and the cut-off frequency of 0.20 Hz. We can also concluded that the 10 best combinations are obtained when the signal length is set at 30 s, so it carries the most valuable information. Depending on the cut-off frequency that is used, best models can be learned when it is between 0.10 Hz and 0.20 Hz. As we mentioned before, in real-life scenarios (e.g., civil and military emergency situations), maybe there is no time to obtain a signal of 30 s, so if we have a signal length of 10 s, using the results reported in Table 5, we can select the best combination when the signal length is 10 s, and this combination is obtained with a cut-off frequency of 0.25 Hz.

We need to mention that the focus here is made on different settings of parameters for pre-processing of ECG signals used for blood pressure classification. Regarding the classification methodology, it could be also tested with some other methodologies; we selected one that was recently published. The novelty in the comparison is that we used a set of 17 performance measures instead of focusing of comparing them separately to the most commonly used performance measures in which a general conclusion is made. The performance measures were selected manually.

5 CONCLUSIONS

We investigated different parameter values that can be used for pre-processing of ECG signals in order to estimate the valuable information that can be further used for blood pressure classification. One parameter is related to the signal length used for data segmentation of the raw ECG signals and the other is related to the cut-off frequency that is applied on each seg-

Table 4: Performance results for best meta-model trained for each combination.

Comb.	ACC	KAPPA	PRC	ROC	F	COR	PR	RC	RAE	RRSE	RMSE	INF	MAR	MF	LL	MI	PRS	Ranking
10/0.05	55.16	0.33	0.54	0.71	0.53	0.32	0.54	0.55	68.23	108.14	0.51	0.31	0.37	0.55	56.59	0.18	96.75	14
10/0.10	46.99	0.24	0.53	0.68	0.45	0.25	0.54	0.47	77.09	109.25	0.54	0.27	0.29	0.47	32.67	0.12	58.12	27
10/0.15	55.30	0.30	0.53	0.70	0.55	0.33	0.56	0.55	66.71	104.72	0.50	0.32	0.34	0.55	40.72	0.19	61.14	16
10/0.20	51.46	0.22	0.51	0.67	0.49	0.23	0.50	0.51	73.99	110.49	0.52	0.24	0.28	0.51	19.38	0.09	29.71	28
10/0.25	54.01	0.31	0.52	0.69	0.54	0.31	0.55	0.54	71.47	110.71	0.52	0.32	0.30	0.54	33.26	0.14	57.64	22
10/0.30	63.14	0.44	0.62	0.78	0.64	0.47	0.68	0.63	58.84	95.76	0.46	0.47	0.45	0.63	52.12	0.22	93.10	1
10/0.35	56.38	0.28	0.60	0.72	0.56	0.32	0.56	0.56	67.75	101.45	0.49	0.32	0.32	0.56	25.18	0.13	40.82	18
10/0.40	50.19	0.24	0.48	0.64	0.50	0.24	0.51	0.50	80.58	116.81	0.55	0.23	0.27	0.50	26.72	0.10	45.47	30
10/0.45	52.68	0.30	0.48	0.66	0.51	0.28	0.52	0.53	75.96	112.93	0.53	0.27	0.34	0.53	32.58	0.15	54.57	24
10/0.50	52.68	0.29	0.49	0.67	0.50	0.28	0.50	0.53	73.16	112.33	0.53	0.27	0.34	0.53	29.21	0.13	49.54	25
20/0.05	56.88	0.35	0.55	0.73	0.54	0.34	0.53	0.57	63.21	106.86	0.51	0.33	0.42	0.57	45.39	0.21	73.83	11
20/0.10	56.07	0.34	0.55	0.72	0.52	0.33	0.53	0.56	69.25	106.40	0.50	0.33	0.42	0.56	48.09	0.20	77.33	12
20/0.15	57.24	0.24	0.57	0.65	0.57	0.23	0.58	0.57	66.19	103.87	0.50	0.23	0.24	0.57	11.33	0.07	20.14	23
20/0.20	57.14	0.32	0.55	0.70	0.57	0.33	0.57	0.57	67.37	104.82	0.50	0.34	0.34	0.57	29.84	0.15	47.90	15
20/0.25	51.64	0.25	0.51	0.66	0.51	0.25	0.52	0.52	75.33	109.22	0.51	0.26	0.23	0.52	26.49	0.11	44.91	26
20/0.30	55.56	0.28	0.58	0.70	0.56	0.30	0.57	0.56	66.80	101.72	0.48	0.30	0.29	0.56	12.89	0.08	20.42	21
20/0.35	65.56	0.37	0.63	0.73	0.65	0.39	0.65	0.66	56.85	94.44	0.46	0.39	0.39	0.66	19.70	0.13	34.84	5
20/0.40	51.03	0.24	0.45	0.61	0.51	0.23	0.51	0.51	78.26	115.49	0.55	0.24	0.22	0.51	39.74	0.10	68.30	29
20/0.45	61.03	0.41	0.58	0.76	0.59	0.41	0.59	0.61	65.11	93.24	0.44	0.41	0.45	0.61	53.41	0.25	86.30	2
20/0.50	54.87	0.33	0.51	0.67	0.55	0.33	0.56	0.55	77.03	103.46	0.49	0.34	0.35	0.55	35.22	0.16	60.30	20
30/0.05	58.64	0.36	0.58	0.75	0.57	0.37	0.56	0.59	61.19	101.95	0.49	0.36	0.40	0.59	70.00	0.24	115.57	7
30/0.10	54.15	0.32	0.53	0.68	0.55	0.34	0.59	0.54	72.85	109.31	0.52	0.35	0.30	0.54	68.93	0.23	115.65	13
30/0.15	60.96	0.41	0.60	0.75	0.62	0.43	0.64	0.61	62.35	97.53	0.47	0.43	0.42	0.61	45.74	0.20	80.81	3
30/0.20	58.48	0.38	0.53	0.69	0.57	0.37	0.58	0.58	67.72	105.90	0.50	0.37	0.41	0.58	47.47	0.21	77.22	10
30/0.25	52.73	0.30	0.54	0.69	0.52	0.34	0.59	0.53	74.38	108.59	0.52	0.36	0.32	0.53	52.02	0.19	88.54	19
30/0.30	56.07	0.33	0.52	0.68	0.56	0.33	0.56	0.56	70.54	105.38	0.50	0.32	0.33	0.56	43.67	0.16	79.52	17
30/0.35	58.37	0.37	0.58	0.74	0.57	0.37	0.57	0.58	64.60	101.66	0.48	0.37	0.40	0.58	49.26	0.22	79.46	9
30/0.40	62.73	0.36	0.59	0.74	0.60	0.43	0.65	0.63	58.09	100.81	0.48	0.48	0.42	0.63	27.00	0.25	40.09	4
30/0.45	59.41	0.38	0.59	0.73	0.59	0.38	0.59	0.59	68.63	100.51	0.47	0.39	0.38	0.59	45.21	0.15	88.38	8
30/0.50	60.48	0.40	0.59	0.74	0.60	0.41	0.60	0.60	68.74	95.42	0.45	0.41	0.41	0.60	37.36	0.18	67.44	6

Table 5: Averaged performance results from all meta-models trained for each combination.

Comb.	ACC	KAPPA	PRC	ROC	F	COR	PR	RC	RAE	RRSE	RMSE	INF	MAR	MF	LL	MI	PRS	Ranking
10/0.05	44.32	0.14	0.45	0.60	0.43	0.14	0.46	0.44	83.80	117.68	0.56	0.14	0.16	0.44	14.64	0.06	24.40	16
10/0.10	43.05	0.12	0.46	0.58	0.43	0.13	0.48	0.43	85.39	119.59	0.57	0.14	0.12	0.43	15.59	0.06	26.19	21
10/0.15	44.02	0.13	0.45	0.59	0.43	0.13	0.46	0.44	84.55	119.00	0.57	0.14	0.14	0.44	14.43	0.06	23.65	19
10/0.20	44.28	0.15	0.44	0.59	0.43	0.15	0.47	0.44	85.16	118.83	0.57	0.16	0.16	0.44	18.22	0.07	30.27	14
10/0.25	45.89	0.15	0.47	0.60	0.45	0.15	0.48	0.46	81.93	116.21	0.55	0.16	0.15	0.46	14.88	0.06	24.46	12
10/0.30	43.78	0.14	0.46	0.60	0.43	0.14	0.47	0.44	83.49	117.40	0.56	0.15	0.14	0.44	15.84	0.06	26.07	15
10/0.35	44.07	0.13	0.46	0.59	0.43	0.14	0.46	0.44	84.54	117.58	0.56	0.13	0.14	0.44	11.94	0.05	18.98	18
10/0.40	42.43	0.11	0.43	0.58	0.41	0.11	0.44	0.42	86.35	120.03	0.57	0.11	0.11	0.42	12.52	0.04	21.03	26
10/0.45	44.51	0.13	0.46	0.59	0.43	0.13	0.45	0.45	83.31	116.29	0.55	0.13	0.15	0.45	10.94	0.05	17.06	17
10/0.50	41.80	0.10	0.44	0.58	0.40	0.10	0.43	0.42	86.91	118.43	0.57	0.10	0.12	0.42	10.41	0.04	16.55	29
20/0.05	42.80	0.13	0.45	0.59	0.42	0.13	0.46	0.43	85.39	118.85	0.57	0.13	0.15	0.43	16.57	0.06	28.14	20
20/0.10	46.08	0.16	0.46	0.59	0.45	0.16	0.49	0.46	81.75	117.28	0.56	0.17	0.17	0.46	18.36	0.06	31.33	11
20/0.15	41.65	0.10	0.44	0.57	0.41	0.11	0.45	0.42	87.05	121.09	0.58	0.12	0.11	0.42	11.59	0.05	18.65	28
20/0.20	42.90	0.12	0.45	0.58	0.42	0.13	0.47	0.43	86.06	118.77	0.57	0.13	0.13	0.43	15.25	0.06	25.31	22
20/0.25	41.97	0.09	0.44	0.57	0.41	0.10	0.45	0.42	86.71	120.46	0.58	0.10	0.10	0.42	11.93	0.05	19.48	30
20/0.30	42.65	0.12	0.44	0.57	0.41	0.11	0.44	0.43	86.93	119.17	0.57	0.12	0.13	0.43	14.81	0.05	24.20	23
20/0.35	41.61	0.10	0.44	0.57	0.40	0.10	0.44	0.42	87.53	120.54	0.58	0.10	0.11	0.42	14.66	0.06	23.60	27
20/0.40	41.76	0.11	0.44	0.57	0.40	0.11	0.45	0.42	87.62	120.57	0.58	0.12	0.12	0.42	15.25	0.06	23.65	25
20/0.45	44.69	0.13	0.47	0.60	0.44	0.14	0.47	0.45	83.58	116.39	0.56	0.15	0.14	0.45	15.72	0.07	24.58	13
20/0.50	42.97	0.10	0.45	0.58	0.42	0.11	0.44	0.43	86.02	118.99	0.57	0.11	0.11	0.43	11.88	0.05	18.69	24
30/0.05	47.96	0.19	0.49	0.62	0.47	0.19	0.50	0.48	78.77	115.69	0.55	0.20	0.21	0.48	23.61	0.09	40.29	5
30/0.10	49.21	0.19	0.49	0.62	0.49	0.20	0.52	0.49	78.07	114.34	0.54	0.21	0.20	0.49	21.45	0.08	36.08	1
30/0.15	47.88	0.20	0.49	0.63	0.47	0.21	0.52	0.48	78.95	114.58	0.55	0.22	0.21	0.48	21.63	0.09	37.32	2
30/0.20	48.21	0.20	0.48	0.62	0.47	0.21	0.51	0.48	79.81	115.27	0.55	0.22	0.22	0.48	24.05	0.10	40.22	3
30/0.25	46.82	0.18	0.48	0.62	0.46	0.18	0.49	0.47	80.50	115.71	0.55	0.19	0.19	0.47	24.06	0.09	40.49	7
30/0.30	45.69	0.16	0.46	0.61	0.44	0.16	0.48	0.46	82.11	116.52	0.56	0.17	0.17	0.46	19.97	0.08	33.25	10
30/0.35	47.53	0.16	0.48	0.60	0.46	0.17	0.50	0.48	79.27	114.75	0.55	0.18	0.16	0.48	19.43	0.08	32.22	8
30/0.40	48.41	0.18	0.48	0.60	0.47	0.18	0.50	0.48	78.94	114.78	0.55	0.19	0.19	0.48	19.29	0.07	32.74	6
30/0.45	48.31	0.18	0.47	0.62	0.47	0.19	0.49	0.48	79.17	114.26	0.54	0.19	0.19	0.48	25.97	0.10	43.66	4
30/0.50	45.79	0.18	0.48	0.63	0.44	0.19	0.50	0.46	82.13	115.70	0.56	0.20	0.21	0.46	19.59	0.07	32.44	9

ment for baseline removal. For this reason, 30 combinations were experimentally evaluated; each one is a combination of different signal length used for data segmentation and cut-off frequency for baseline removal. For the signal lengths: 10 s, 20 s, and 30 s, were used; while the cut-off frequency starts from 0.05 Hz, till 0.50 Hz, with a step of 0.05 Hz.

The evaluation of these combinations was performed in a combination with complexity analysis used for feature extraction that are further used for blood pressure classification. The evaluation was done using a dataset that contains data from five commercially available ECG sensors. The dataset was

pre-processed for each combination separately. The same classification methodology was used for each pre-processed dataset, which results are only used to estimate the valuable information that these combinations convey. A data-driven methodology from multi-criteria decision analysis was used to rank these combinations regarding a set of 17 performance measures.

Evaluation results showed that the best results can be achieved using a signal length of 30 s, so it follows that it carries the most valuable information. Regarding the cut-off frequency, it follows that good models are achieved when it is between 0.10 Hz and 0.20 Hz. This is a contribution to the arguments pub-

lished in the literature discussing the optimal ECG sample lengths needed for building predictive models (Takahashi et al., 2017; Shdefat et al., 2018), as well as the lower frequencies where the ECG components overlap with the baseline wander noise (Xu et al., 2017). Also, this analysis can further give additional directions for research, where the pre-processing will not be made regarding a fix signal length and cut-off frequency for baseline removal, but it can produce information that can be used for information fusion approaches.

ACKNOWLEDGEMENTS

This work was supported by the Slovenian Research Agency (research core funding No. P2-0098, and project J1-8155), and by SIARS, NATO multi-year project NATO.EAP.SFPP 984753.

REFERENCES

- AHA (2016). Understanding blood pressure readings.
- Ahmad, S., Chen, S., Soueidan, K., Batkin, I., Bolic, M., Dajani, H., and Groza, V. (2012). Electrocardiogram-assisted blood pressure estimation. *IEEE Transactions on Biomedical Engineering*, 59(3):608–618.
- Ahonen, L., Cowley, B., Torniaainen, J., Ukkonen, A., Vihavainen, A., and Puolamäki, K. (2016). Cognitive collaboration found in cardiac physiology: Study in classroom environment. *PLoS one*, 11(7):e0159178.
- Biosignals, B. (2016). Emotion faros (2016).
- Brans, J.-P. and Mareschal, B. (2005). Promethee methods. In *Multiple criteria decision analysis: state of the art surveys*, pages 163–186. Springer.
- Breiman, L. (1996). Bagging predictors. *Machine learning*, 24(2):123–140.
- Canning, J., Helbert, K., Iashin, G., Matthews, J., Yang, J., Delano, M. K., Sodini, C. G., and Zhang, Q. (2016). Noninvasive and continuous blood pressure measurement via superficial temporal artery tonometry. In *Engineering in Medicine and Biology Society (EMBC), 2016 IEEE 38th Annual International Conference of the*, pages 3382–3385. IEEE.
- Chan, K., Hung, K., and Zhang, Y. (2001). Noninvasive and cuffless measurements of blood pressure for telemedicine. In *Engineering in Medicine and Biology Society, 2001. Proceedings of the 23rd Annual International Conference of the IEEE*, volume 4, pages 3592–3593. IEEE.
- Choi, Y., Zhang, Q., and Ko, S. (2013). Noninvasive cuffless blood pressure estimation using pulse transit time and hilbert–huang transform. *Computers & Electrical Engineering*, 39(1):103–111.
- Cosoli, G., Casacanditella, L., Pietroni, F., Calvaresi, A., Revel, G. M., and Scalise, L. (2015). A novel approach for features extraction in physiological signals. In *Medical Measurements and Applications (MeMeA), 2015 IEEE International Symposium on*, pages 380–385. IEEE.
- Eftimov, T., Korošec, P., and Seljak, B. K. (2018). Data-driven preference-based deep statistical ranking for comparing multi-objective optimization algorithms. In *International Conference on Bioinspired Methods and Their Applications*, pages 138–150. Springer.
- Eke, A., Herman, P., Kocsis, L., and Kozak, L. (2002). Fractal characterization of complexity in temporal physiological signals. *Physiological measurement*, 23(1):R1.
- Freund, Y., Schapire, R. E., et al. (1996). Experiments with a new boosting algorithm. In *Icml*, volume 96, pages 148–156. Citeseer.
- Goldberger, A. L., Amaral, L. A., Glass, L., Hausdorff, J. M., Ivanov, P. C., Mark, R. G., Mietus, J. E., Moody, G. B., Peng, C.-K., and Stanley, H. E. (2000). PhysioBank, physioToolkit, and physionet. *Circulation*, 101(23):e215–e220.
- Goli, S. and Jayanthi, T. (2014). Cuff less continuous non-invasive blood pressure measurement using pulse transit time measurement. *International Journal of Recent Development in Engineering and Technology*, 2(1):87.
- Hacks, C. (2015). e-health sensor platform v2. 0 for arduino and raspberry pi.
- Hassan, M. K. B. A., Mashor, M., Nasir, N. M., and Mohamed, S. (2008). Measuring of systolic blood pressure based on heart rate. In *4th Kuala Lumpur International Conference on Biomedical Engineering 2008*, pages 595–598. Springer.
- Hearst, M. A., Dumais, S. T., Osuna, E., Platt, J., and Scholkopf, B. (1998). Support vector machines. *IEEE Intelligent Systems and their applications*, 13(4):18–28.
- i Carós, J. M. S. (2011). *Continuous non-invasive blood pressure estimation*. PhD thesis, ETH.
- Ilango, S. and Sridhar, P. (2014). A non-invasive blood pressure measurement using android smart phones. *IOSR Journal of Dental and Medical Sciences*, 13(1):28–31.
- Johnstone, J. A., Ford, P. A., Hughes, G., Watson, T., and Garrett, A. T. (2012). Bioharness™ multivariable monitoring device: part. i: validity. *Journal of sports science & medicine*, 11(3):400.
- Kim, N., Krasner, A., Kosinski, C., Winger, M., Qadri, M., Kappus, Z., Danish, S., and Craelius, W. (2016). Trending autoregulatory indices during treatment for traumatic brain injury. *Journal of clinical monitoring and computing*, 30(6):821–831.
- Kugiumtzis, D. and Tsimpiris, A. (2010). Measures of analysis of time series (mats): A matlab toolkit for computation of multiple measures on time series data bases. *arXiv preprint arXiv:1002.1940*.
- Li, Y., Gao, Y., and Deng, N. (2013). Mechanism of cuffless blood pressure measurement using mmsb. *Engineering*, 5(10):123.
- Liao, Y. and Vemuri, V. R. (2002). Use of k-nearest neigh-

- bor classifier for intrusion detection1. *Computers & security*, 21(5):439–448.
- Liaw, A., Wiener, M., et al. (2002). Classification and regression by randomforest. *R news*, 2(3):18–22.
- Marani, R. and Perri, A. G. (2012). An intelligent system for continuous blood pressure monitoring on remote multi-patients in real time. *arXiv preprint arXiv:1212.0651*.
- McBride, J. C., Zhao, X., Munro, N. B., Smith, C. D., Jicha, G. A., Hively, L., Broster, L. S., Schmitt, F. A., Kryscio, R. J., and Jiang, Y. (2014). Spectral and complexity analysis of scalp eeg characteristics for mild cognitive impairment and early alzheimer’s disease. *Computer methods and programs in biomedicine*, 114(2):153–163.
- Monge-Álvarez, J. (2015). Higuchi and katz fractal dimension measures. https://www.mathworks.com/matlabcentral/fileexchange/50290-higuchi-and-katz-fractal-dimension-measures/content/Fractal_dimension_measures/Higuchi_FD.m.
- Morabito, F. C., Labate, D., La Foresta, F., Bramanti, A., Morabito, G., and Palamara, I. (2012). Multivariate multi-scale permutation entropy for complexity analysis of alzheimer’s disease eeg. *Entropy*, 14(7):1186–1202.
- Mouradian, V., Poghosyan, A., and Hovhannisyanyan, L. (2015). Noninvasive continuous mobile blood pressure monitoring using novel ppg optical sensor. In *Biomedical Wireless Technologies, Networks, and Sensing Systems (BioWireless)*, 2015 IEEE Topical Conference on, pages 1–3. IEEE.
- Nitzan, M. (2011). Automatic noninvasive measurement of arterial blood pressure. *IEEE instrumentation & measurement magazine*, 14(1).
- Nye, R., Zhang, Z., and Fang, Q. (2015). Continuous non-invasive blood pressure monitoring using photoplethysmography: A review. In *Bioelectronics and Bioinformatics (ISBB)*, 2015 International Symposium on, pages 176–179. IEEE.
- Patil, T. R. and Shrekar, S. (2013). Performance analysis of naive bayes and j48 classification algorithm for data classification. *International journal of computer science and applications*, 6(2):256–261.
- Payne, R., Symeonides, C., Webb, D., and Maxwell, S. (2006). Pulse transit time measured from the ECG: an unreliable marker of beat-to-beat blood pressure. *Journal of Applied Physiology*, 100(1):136–141.
- Powers, D. M. (2011). Evaluation: from precision, recall and f-measure to roc, informedness, markedness and correlation.
- Program, N. H. B. P. E. et al. (2004). The seventh report of the joint national committee on prevention, detection, evaluation, and treatment of high blood pressure.
- Rish, I. et al. (2001). An empirical study of the naive bayes classifier. In *IJCAI 2001 workshop on empirical methods in artificial intelligence*, volume 3, pages 41–46. IBM New York.
- Sackl-Pietsch, E. (2010). Continuous non-invasive arterial pressure shows high accuracy in comparison to invasive intra-arterial blood pressure measurement. *Unpublished manuscript*.
- Sahani, A. K., Ravi, V., and Sivaprakasam, M. (2014). Automatic estimation of carotid arterial pressure in ar- sens. In *India Conference (INDICON), 2014 Annual IEEE*, pages 1–6. IEEE.
- Sahoo, A., Manimegalai, P., and Thanushkodi, K. (2011). Wavelet based pulse rate and blood pressure estimation system from ECG and PPG signals. In *Computer, Communication and Electrical Technology (ICCCET), 2011 International Conference on*, pages 285–289. IEEE.
- Schroeder, E. B., Liao, D., Chambless, L. E., Prineas, R. J., Evans, G. W., and Heiss, G. (2003). Hypertension, blood pressure, and heart rate variability. *Hypertension*, 42(6):1106–1111.
- Seo, J., Pietrangelo, S. J., Lee, H.-S., and Sodini, C. G. (2015). Noninvasive arterial blood pressure waveform monitoring using two-element ultrasound system. *IEEE transactions on ultrasonics, ferroelectrics, and frequency control*, 62(4):776–784.
- Shdefat, A. Y., Joo, M.-I., Choi, S.-H., and Kim, H.-C. (2018). Utilizing ECG waveform features as new biometric authentication method. *International Journal of Electrical and Computer Engineering (IJECE)*, 8(2).
- Shriram, R., Wakankar, A., Daimiwal, N., and Ramdasi, D. (2010). Continuous cuffless blood pressure monitoring based on ptt. In *Bioinformatics and Biomedical Technology (ICBBT), 2010 International Conference on*, pages 51–55. IEEE.
- Simjanoska, M., Gjoreski, M., Gams, M., and Madevska Bogdanova, A. (2018). Non-invasive blood pressure estimation from ECG using machine learning techniques. *Sensors*, 18(4):1160.
- Takahashi, N., Kuriyama, A., Kanazawa, H., Takahashi, Y., and Nakayama, T. (2017). Validity of spectral analysis based on heart rate variability from 1-minute or less ECG recordings. *Pacing and Clinical Electrophysiology*.
- Tanaka, S., Nogawa, M., Yamakoshi, T., and Yamakoshi, K.-i. (2007). Accuracy assessment of a noninvasive device for monitoring beat-by-beat blood pressure in the radial artery using the volume-compensation method. *IEEE Transactions on Biomedical Engineering*, 54(10):1892–1895.
- Technology, Z. (2017). Zephyr bioharness 3.0 user manual. <https://www.zephyranywhere.com/media/download/bioharness3-user-manual.pdf>.
- Thomas, S. S., Nathan, V., Zong, C., Soundarapandian, K., Shi, X., and Jafari, R. (2016). Biowatch: A noninvasive wrist-based blood pressure monitor that incorporates training techniques for posture and subject variability. *IEEE journal of biomedical and health informatics*, 20(5):1291–1300.
- Trobec, R., Tomašić, I., Rashkovska, A., Depolli, M., and Avbelj, V. (2018a). Commercial eeg systems. In *Body Sensors and Electrocardiography*, pages 101–114. Springer.

- Trobec, R., Tomašić, I., Rashkovska, A., Depolli, M., and Avbelj, V. (2018b). Commercial ECG systems. In *Body Sensors and Electrocardiography*, pages 101–114. Springer.
- Vihinen, M. (2012). How to evaluate performance of prediction methods? measures and their interpretation in variation effect analysis. In *BMC genomics*, volume 13, page S2. BioMed Central.
- Winderbank-Scott, P. and Barnaghi, P. (2017). A non-invasive wireless monitoring device for children and infants in pre-hospital and acute hospital environments.
- Wong, M. Y.-M., Poon, C. C.-Y., and Zhang, Y.-T. (2009). An evaluation of the cuffless blood pressure estimation based on pulse transit time technique: a half year study on normotensive subjects. *Cardiovascular Engineering*, 9(1):32–38.
- Xu, Y., Luo, M., Li, T., and Song, G. (2017). Ecg signal de-noising and baseline wander correction based on ceemdan and wavelet threshold. *Sensors*, 17(12):2754.
- Zhang, X.-Y. and Zhang, Y.-T. (2006). A model-based study of relationship between timing of second heart sound and systolic blood pressure. In *Engineering in Medicine and Biology Society, 2006. EMBS'06. 28th Annual International Conference of the IEEE*, pages 1387–1390. IEEE.
- Zhou, P., Zong-Xia, M., Chun-Lan, H., and Huang, Y.-X. (2017). Power spectral entropy in the ECG of patients suffered from nocturnal frontal lobe epilepsy. *Journal of Pharmaceutical and Biomedical Sciences*, 7(3).